

Energy decomposition analysis of neutral and negatively charged borophenes

T. Tarkowski, J. A. Majewski, N. Gonzalez Szwacki*

Institute of Theoretical Physics, Faculty of Physics, University of Warsaw, Pasteura 5, PL-02093 Warszawa, Poland

Abstract

The effect of external static charging on borophenes – 2D boron crystals – is investigated by using first principles calculations. The influence of the excess negative charge on the stability of the 2D structures is examined using a very simple analysis of decomposition of the binding energy of a given boron layer into contributions coming from boron atoms that have different coordination numbers. This analysis is important to understand how the local neighbourhood of an atom influences the overall stability of the monolayer structure. The decomposition is done for the α -sheet and its related family of structures. From this analysis, we have found a preference for 2D boron crystals with very small or very high charges per atom. The structures with intermediate charges are energetically not favourable. We have also found a clear preference in terms of binding energy for the experimentally seen γ -sheet and δ -sheet structures that is almost independent on the considered excess of negative charge of the structures. On the other hand, we have shown that a model based solely on nearest-neighbour interactions, although instructive, is too simple to predict binding energies accurately.

Keywords: *ab initio* calculations, borophene, energy decomposition

PACS: 31.15.A-, 31.15.es, 61.46.-w, 62.23.Kn, 62.25.-g, 68.65.-k

1. Introduction

Like carbon, boron can adopt bonding configurations that favor the formation of low-dimensional structures such as nanotubes, fullerenes, and sheets. With these different forms (or allotropes) could come interesting and novel properties distinct from those of the bulk structures. Two-dimensional (2D) allotropes of boron have been studied theoretically more extensively during the last ten years [1]. There are different proposals based on first principles calculations for the atomic structure of 2D boron crystals: buckled triangular (bt) sheet [2, 3, 4], α -sheet and related planar and quasiplanar layers [5, 6, 7, 8], non-zero thick layers and bilayers [9, 10, 11], B_{12} -based layers [9], and other structures [12, 7]. However, the experimental realization came just recently and confirmed only some of those structures.

G. Tai *et al.* [13] reported the synthesis of 2D boron structures on copper foils by chemical vapor deposition (CVD), by combining boron and B_2O_3 to make B_2O_2 vapour and reducing it with hydrogen while passing it over copper foil. Their 2D boron structure consists of B_{12} icosahedra held together by B_2 dumbbells and behaves as a direct band gap semiconductor. The same year, Manix *et al.* [14] reported the synthesis of 2D boron sheets grown on a single crystal Ag(111) substrate using molecular beam epitaxy (MBE) under ultrahigh-vacuum (UHV)

conditions. Two distinct forms of 2D boron structures have been observed, both consisting of triangular layers with some fraction of missing atoms (empty hexagons, hexagonal holes or vacancies) in the hexagonal lattice. In one form (labeled in this work as γ -sheet, see Fig. 1b) rows of filled hexagons are separated by chains of empty hexagons; in the other (labeled in this work as δ -sheet, see Fig. 1b), boron atoms take up narrow zigzag stripes separated by arrays of empty hexagons. Should be noted that the first form was initially proposed to be the bt sheet (see Fig. 1a) [14], and then recently confirmed to be the γ -sheet [15]. Similarly, Feng *et al.* [16] used MBE to grow 2D sheets of boron on a metallic Ag(111) substrate by direct evaporation of a pure boron source under UHV conditions. They also observed two different structures corresponding to the described above γ and δ sheets. According to this study, both sheets are flat, metallic in character, and quite stable against oxidation in air. Moreover, the sheets appear to be robust and only weakly bound to their substrate, indicating that it might be possible to obtain freestanding sheets, but the question of how to detach the sheets from the substrates is still open. Finally, in the most recent experimental study [17] two reproducible metallic phases of 2D boron are found on Ag(111), one of them being the γ -sheet and the other one presumably being the α -sheet. All these experimental studies pave the way to fascinating applications in nanoelectronic and nanophotonic devices [1, 13, 18].

*Corresponding author.

Email address: gonz@fuw.edu.pl (N. Gonzalez Szwacki)

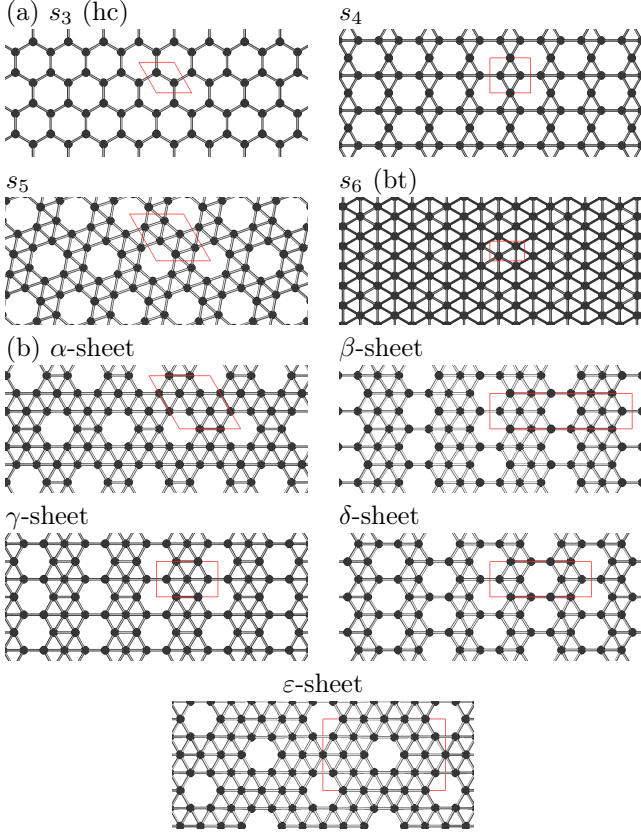


Figure 1: (Color online). 2D boron layers considered in this study. (a) Structures that are used to calculate the values of the e_s energies in our model. (b) Structures that are used to test the accuracy of our model. In all cases, the conventional unit cells are shown in red.

There are still many unanswered questions about the structure and properties of 2D boron structures. In this work, we concentrate only on monolayer boron structures. For these structures it is not clear, for instance, why from the vast number of distinct 2D boron sheets reported theoretically [18], only some of them seem to be favored and realized experimentally. Also, the high-symmetry α -sheet that has been predicted to be one of the most stable one-atom-thick forms of 2D boron is believed to be obtained just very recently [17]. As of our understanding, the main factors that may influence the structure of 2D boron crystals are the strain induced by the substrate and the amount of negative charge that is transferring from the substrate [18]. In this study, we propose a simple model to predict the structure of 2D boron crystals exposed to static negative charge. The model does not include the strain but may serve as a first step in the search for stable charged boron sheets.

2. Computational approach

Our first principles calculations are based on density functional theory (DFT) and the projector augmented wave (PAW) method as implemented in the QUANTUM ESPRESSO simulation package [19]. For the exchange and

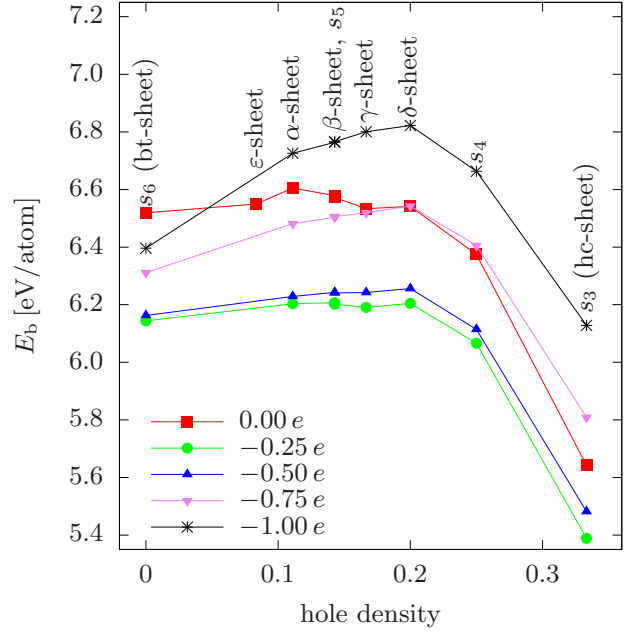


Figure 2: (Color online). Binding energy versus hole density for neutral and negatively charged boron sheets. The two limiting cases of 0 and $1/3$ hole density correspond to the buckled triangular and honeycomb sheets, respectively. Maximum E_b occurs for sheets α and δ for neutral and charged structures, respectively. Two structures, β -sheet and s_5 , have the same hole density values and a slightly different (by few meV) binding energy per atom.

correlation functional, we use a revised Perdew-Burke-Ernzerhof spin-polarized generalized gradient approximation (PBEsol-GGA) functional. The plane-wave basis set is converged using a 60 Ry energy cutoff. A $8 \times 8 \times 1$ \mathbf{k} -point mesh and a Gaussian smearing of 0.005 Ry is used in the Brillouin Zone integration. The calculations are done using supercells ensuring a 50 Å separation between adjacent layers. For the charged structures, the amount of negative charge (excess of electrons) is specified in units of the charge of an electron per boron atom. For each considered structure, we do a full atomic position and lattice parameter relaxation. The 2D bulk modulus for the hc-sheet (s_3) is obtained from the Murnaghan equation of state.

Images of the crystal structures shown in Fig. 1 were created using the VESTA visualization program [20]. The space group symmetries are found by using the FINDSYM software package [21] and later on reduced to plane group symmetries. The \mathbf{k} -point mesh used in the density of states (DOS) and charge density post-processing calculations was $10 \times 10 \times 1$.

3. Results and discussion

3.1. Static charging of 2D boron structures

The structure of all the theoretically and experimentally reported one-atom-thick 2D boron crystals can be

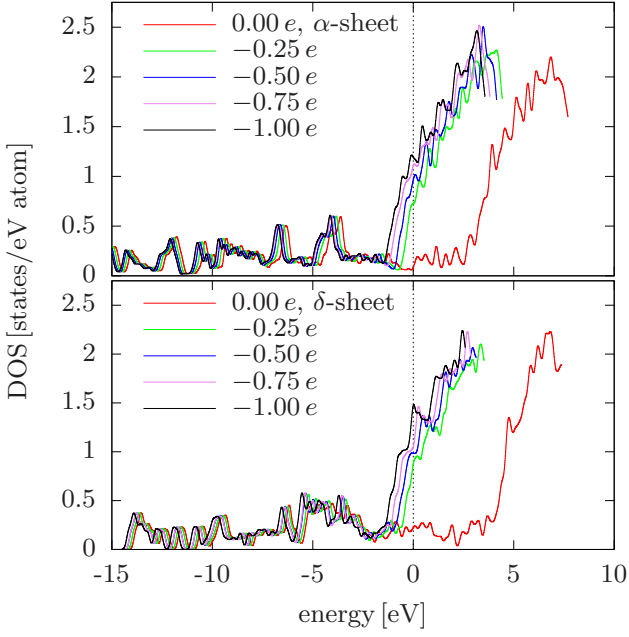


Figure 3: (Color online). Density of states for neutral and negatively charged α (top) and δ (bottom) sheets. The zero of energy is set to the Fermi level.

easily compared to that of graphene, with that difference that part of the hexagons in the boron layers are filled with additional boron atoms. Should be pointed out that the α , γ , and δ sheets with periodic arrangements of empty hexagons have been extensively studied theoretically either as freestanding structures or on metallic and nonmetallic substrates long before the actual experimental realization of these structures [22, 23, 24, 25, 26]. In the extreme case of all the hexagons filled with atoms, we get the bt-sheet mentioned above that was extensively studied theoretically at the earliest stage of the 2D boron investigation [2, 3, 4]. On the other hand, the boron sheet with honeycomb (hc) structure is unstable with respect to shearing perturbations [2]. However, for the purpose of our analysis, we fix the symmetry of the boron hc-sheet during relaxation in order to preserve its structure. We define the hexagon hole density of the boron layer in the same way as in Ref. [5], namely as the ratio between the number of missing B atoms in the triangular sheet and the number of atoms in the fully filled sheet. In that way, the bt and hc sheets have hexagon hole densities equal to 0 and 1/3, respectively. The full set of structures, with different hole densities considered in this work, is shown in Fig. 1.

In Fig. 2, we have plotted the dependence of the binding energy, $E_b = E_{\text{tot}}(\text{isolated B atom}) - E_{\text{tot}}(\text{B layer})/N$, where E_{tot} is the computed total energy and N is the number of atoms in the supercell, versus the hexagon hole density for structures with different static charges q . For neutral structures, the picture is the same as reported in Ref. [5], however, it is clear from this figure that static

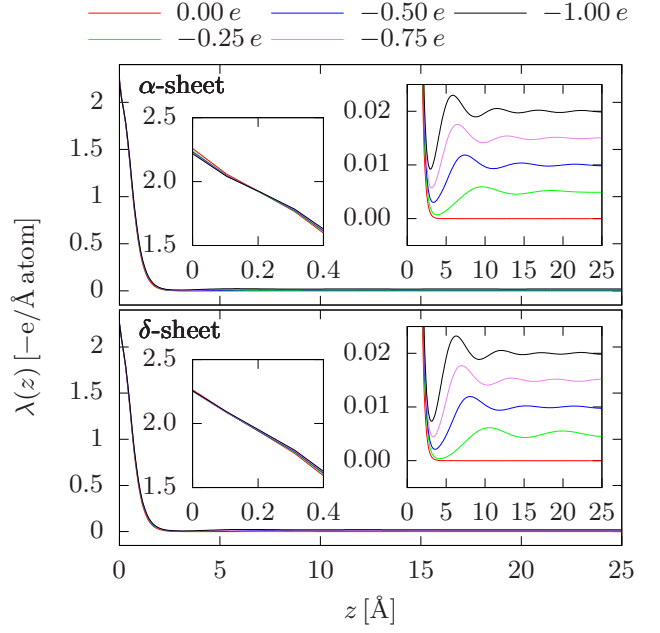


Figure 4: (Color online). Planarly averaged charge density $\lambda(z) = \frac{1}{N} \int_{V_{2D}} \frac{\partial^3 Q}{\partial x \partial y \partial z} dx dy$, where N is the number of atoms in the unit cell of volume V_{2D} , for neutral and negatively charged α (top) and δ (bottom) sheets. The insets show close-ups of the relevant regions of the charge density distributions.

negative charge gives preference in terms of energy to the δ -sheet and next, for $|q| > 0.25$ e/atom, to the γ -sheet, that is, to structures that were recently reported experimentally [16]. Interestingly enough, almost all 2D layers studied here have the smallest and the largest E_b values for $q = -0.25$ e/atom and $q = -1.00$ e/atom, respectively. The exception is the bt-sheet that has the largest E_b for the neutral structure. In Fig. 2, we can also see that for $|q| \leq 0.5$ e/atom, there is a small dependence of E_b on the hexagon hole density for structures with hole densities ranging from 0 to 0.2. On the other hand, for the highly charged case of $q = -1.00$ e/atom, there is a well defined maximum in E_b that corresponds to the δ -sheet.

The DOS for the neutral and charged α and δ sheets is plotted in Fig. 3. For the neutral structures, it is clear that the α -sheet has a slightly smaller DOS at the Fermi level making this structure, in principle, more stable but less conductive. Our DOS calculations and also those reported in the literature [22, 6, 7] predict a metallic behavior for the γ -sheet and all the other considered in this work 2D structures. Should be mentioned, however, that calculations using the PBE0 hybrid functional anticipate that the α -sheet is a semiconductor [8]. In the case of the charged boron sheets, the excess of negative charge populates the surface states even for the smallest considered negative charge. This is shown in Fig. 3 top and bottom on the example of the α and δ sheets, respectively. A similar picture was reported for static charging of graphene [27]

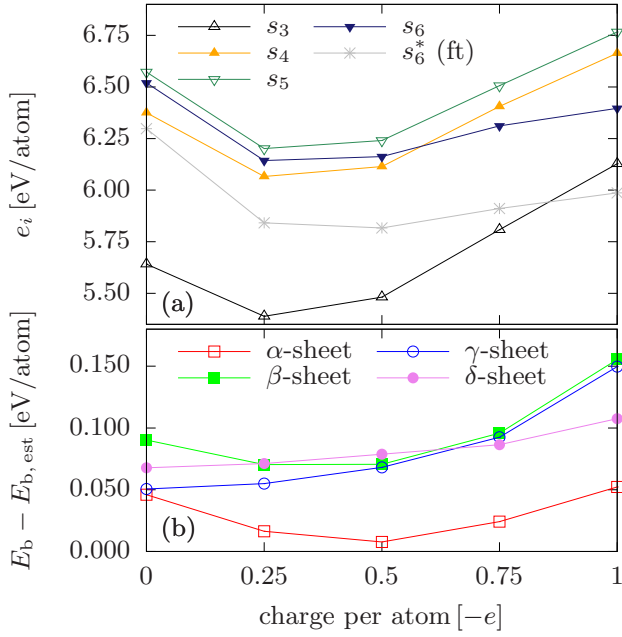


Figure 5: (Color online). (a) Individual energy contributions, e_i , used in our model versus the excess of negative charge. The e_i energies are binding energies per atom of structures with only one type of coordination number i , shown in Fig. 1a. (b) Difference between calculated, E_b , and estimated (from the model), $E_{b, est}$, binding energies plotted as a function of the excess of negative charge for the structures shown in Fig. 1b.

for which the surface states get occupied with electrons for charges as small as $q = -0.0115$ e/atom.

The real-space planarly averaged valence charge density distribution for the neutral and charged α and δ sheets is shown in Fig. 4 top and bottom, respectively. As can be seen in the figure, the charge distributions for those two structures are almost identical (see the insets of the figure). For the neutral structures, the charge density is nearly entirely localized within ~ 2.5 Å at both sides from the layers. The relevant portion of the excess of negative charge is distributed from ~ 2.5 Å to about 15 Å from the layers (see the right insets of Fig. 4). It is interesting to note that the negative charge gets closer towards the planar structures with the increase of excess of charge. For each considered case, there is also a small portion of negative charge distributed practically evenly across the vacuum region of the cells, what is an artifact of our periodic DFT calculations. A similar picture extends also for the rest of the considered structures.

3.2. Energy decomposition analysis

To understand the results presented in Fig. 2, we propose a simple model in which we decompose the binding energy of 2D boron crystals into contributions of energies of the constituent atoms that have different coordination numbers. For that purpose, we express the binding energy

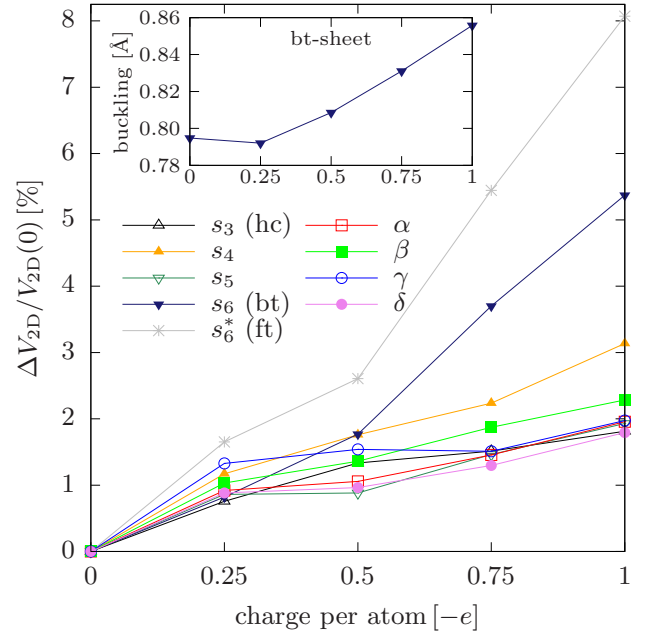


Figure 6: (Color online). Expansion of the unit cell 2D volume versus excess charge per atom. For each considered structure, the values are given relative to the 2D volume of the corresponding neutral structure. Inset: Buckling of the bt-sheet versus excess of negative charge per atom.

of each structure as:

$$E_b(n_3, n_4, n_5, n_6, q) = \frac{1}{N} \sum_{i=3}^6 n_i e_i(q),$$

where n_i and e_i are the number of boron atoms in the unit cell with i nearest neighbors and their energy, respectively, and N is the total number of atoms per unit cell. The individual energy contributions, e_i , are found from separate computations for structures with only one type of coordination number i . The idea is to have $E_b(n_i, q)$ for several structures and compare the results with first principles calculations. The dependence of the e_i energies on charge q is shown in Fig. 5a, whereas the comparison between the predicted and calculated binding energies for each considered charge is shown in Fig. 5b. As can be seen from Fig. 5b this model is too simple to predict the binding energies of 2D boron structures, i.e., the difference between the estimated and computed binding energies is for each neutral structure quite large and changes with the excess of negative charge. This might imply that the interactions between an atom and its second and more distant nearest neighbors should be also included in order to describe correctly the binding energy of neutral and charged structures. From Fig. 5a, we can learn, however, that the s_4 , s_5 , and s_6 (bt-sheet) are the most energetically favorable structures (for neutral and negative charges) among those considered to build the model. Therefore, despite the limitations, based on our model we may conclude that

Table 1: Structural properties of the neutral structures shown in Fig. 1. In the table, V_{2D} represents the 2D volume per atom and N the number of atoms in the conventional unit cell of dimensions a , b . For each structure, its binding energy, E_b , is also provided.

	α	β	γ	δ	ε	s_3 (hc)	s_4	s_5	s_6 (bt)	s_6^* (ft)
plane group	$p6mm$	cmm	pmm	cmm	cmm	$p6mm$	pmm	$p6$	pmm	$p6mm$
a [Å]	5.0494	11.7674	5.0628	8.4017	10.1386	2.9098	3.3528	4.4576	2.8636	1.6985
b [Å]	5.0494	2.9291	2.9120	2.9012	5.8562	2.9098	2.8729	4.4576	1.6247	1.6985
buckling	0	0	0	0	0.1861	0	0	0	0.7948	0
V_{2D} [Å ² /atom]	2.76	2.87	2.95	3.05	2.70	3.67	3.21	2.87	2.33	2.50
N	8	12	5	8	22	2	3	6	2	1
hole density	1/9	1/7	1/6	1/5	1/12	1/3	1/4	1/7	0	0
E_b [eV/atom]	6.6050	6.5791	6.5333	6.5413	6.5498	5.6419	6.3749	6.5723	6.5193	6.2976

the most stable neutral and negatively charged flat boron sheets should be those that have the largest number of four- and five-coordinated B atoms, and this is actually the case of the experimentally obtained δ -sheet. On the other hand, the s_3 structure (hc-sheet) is the least favorable – it is even worse than the ft-sheet for all the considered cases (with the exception of $q = -1.00$ e/atom). This means that boron layers that have tree-coordinated atoms should be the least stable.

3.3. Structural properties

In Tab. 1, we summarize structural properties of the investigated structures. All of the structures described there, with the exception of s_6 (bt-sheet) and ε -sheet, are fully planar, i.e. only s_6 and ε exhibit periodic vertical displacements (buckling) of the atoms. Moreover, the s_6 -sheet does not have 6-fold rotation point – this symmetry is broken due to crystal deformation of the flat triangular lattice.

It is interesting to mention that boron will not adopt the honeycomb structure even if charged with negative charges as high as -1.00 e/atom. This is clear not only from the perspective of the binding energy for the hc-sheet that is always smaller than that of the, e.g., bt-sheet (see Fig. 2), but also the hc-sheet will undergo distortions if the symmetry constrain is removed. Moreover, the 2D bulk modulus of the highly charged hc-sheet is 81 N/m (74.1 N/m, for the neutral structure), what is closer in value to that of neutral silicene (72.00 N/m, taken from Ref. [28]) than that of neutral graphene (211.8 N/m).

Finally, in Fig. 6, we show the expansion of the unit cell 2D volume versus excess of negative charge. From that figure we see that the largest expansion with increasing negative charge occurs for the flat-triangular sheet (followed by the bt-sheet), whereas the variation in 2D volume is much smaller for structures with hexagonal holes. Similarly, in the case of graphene, negative charging has little effect on its lattice constant, since the excess of electrons mostly go away from the structure [27].

4. Conclusions

The performed studies reveal that there is a clear preference for 2D boron structures with very small or very high

negative charge per atom. Structures with intermediate charges are energetically not favorable. Our analysis also suggests that under electron rich conditions there should be a clear preference for the formation of the δ -sheet, since this structure exhibits the highest binding energy and is composed purely of four- and five-coordinated B atoms. Any static charging seems to be detrimental in terms of binding energy for the bt-sheet, however, this structure undergoes the second highest (after the ft-sheet) 2D volume expansion from all the considered boron sheets, what may be helpful in matching to the size of the unit cell of the metallic substrate.

Acknowledgements

The authors gratefully acknowledge the support of the National Research Council (NCN) through the grant UMO-2013/11/B/ST3/04273. Numerical calculations were performed at ICM at the University of Warsaw under grant No. G62-8.

References

- [1] X.-B. Li, S.-Y. Xie, H. Zheng, W. Q. Tian, H.-B. Sun, Boron based two-dimensional crystals: theoretical design, realization proposal and applications, *Nanoscale* 7 (2015) 18863. doi:10.1039/C5NR04359J.
- [2] M. H. Evans, J. D. Joannopoulos, S. T. Pantelides, Electronic and mechanical properties of planar and tubular boron structures, *Physical Review B* 72 (2005) 045434. doi:10.1103/PhysRevB.72.045434.
- [3] J. Kunstmann, A. Quandt, Broad boron sheets and boron nanotubes: An *ab initio* study of structural, electronic, and mechanical properties, *Physical Review B* 74 (2006) 035413. doi:10.1103/PhysRevB.74.035413.
- [4] I. Cabria, M. J. López, J. A. Alonso, Density functional calculations of hydrogen adsorption on boron nanotubes and boron sheets, *Nanotechnology* 17 (2006) 778. doi:10.1088/0957-4484/17/3/027.
- [5] H. Tang, S. Ismail-Beigi, Novel precursors for boron nanotubes: The competition of two-center and three-center bonding in boron sheets, *Physical Review Letters* 99 (2007) 115501. doi:10.1103/PhysRevLett.99.115501.
- [6] E. S. Penev, S. Bhowmick, A. Sadrzadeh, B. I. Yakobson, Polymorphism of two-dimensional boron, *Nano Letters* 12 (5) (2012) 2441–2445. doi:10.1021/nl3004754.

- [7] X. Yu, L. Li, X.-W. Xu, C.-C. Tang, Prediction of two-dimensional boron sheets by particle swarm optimization algorithm, *The Journal of Physical Chemistry C* 116 (37) (2012) 20075–20079. doi:10.1021/jp305545z.
- [8] X. Wu, J. Dai, Y. Zhao, Z. Zhuo, J. Yang, X. C. Zeng, Two-dimensional boron monolayer sheets, *ACS Nano* 6 (8) (2012) 7443–7453. doi:10.1021/nn302696v.
- [9] K. C. Lau, R. Pandey, Stability and electronic properties of atomistically-engineered 2d boron sheets, *The Journal of Physical Chemistry C* 111 (7) (2007) 2906–2912. doi:10.1021/jp066719w.
- [10] X.-F. Zhou, X. Dong, A. R. Oganov, Q. Zhu, Y. Tian, H.-T. Wang, Semimetallic two-dimensional boron allotrope with massless dirac fermions, *Physical Review Letters* 112 (2014) 085502. doi:10.1103/PhysRevLett.112.085502.
- [11] F. Ma, Y. Jiao, G. Gao, Y. Gu, A. Bilic, Z. Chen, A. Du, Graphene-like two-dimensional ionic boron with double dirac cones at ambient condition, *Nano Letters* 16 (5) (2016) 3022–3028. doi:10.1021/acs.nanolett.5b05292.
- [12] N. Gonzalez Szwacki, Boron fullerenes: A first-principles study, *Nanoscale Research Letters* 3 (2) (2007) 49. doi:10.1007/s11671-007-9113-1.
- [13] G. Tai, T. Hu, Y. Zhou, X. Wang, J. Kong, T. Zeng, Y. You, Q. Wang, Synthesis of atomically thin boron films on copper foils, *Angewandte Chemie International Edition* 54 (2015) 15473. doi:10.1002/anie.201509285.
- [14] A. J. Mannix, X.-F. Zhou, B. Kiraly, J. D. Wood, D. Al-ducin, B. D. Myers, X. Liu, B. L. Fisher, U. Santiago, J. R. Guest, M. J. Yacaman, A. Ponce, A. R. Oganov, M. C. Hersam, N. P. Guisinger, Synthesis of borophenes: Anisotropic, two-dimensional boron polymorphs, *Science* 350 (2015) 1513. doi:10.1126/science.aad1080.
- [15] Z. Zhang, A. J. Mannix, Z. Hu, B. Kiraly, N. P. Guisinger, M. C. Hersam, B. I. Yakobson, Substrate-induced nanoscale undulations of borophene on silver, *Nano Letters* 16 (10) (2016) 6622–6627. doi:10.1021/acs.nanolett.6b03349.
- [16] B. Feng, J. Zhang, Q. Zhong, W. Li, S. Li, H. Li, P. Cheng, S. Meng, L. Chen, K. Wu, Experimental realization of two-dimensional boron sheets, *Nature Chemistry* 8 (2016) 563. doi:10.1038/nchem.2491.
- [17] Q. Zhong, J. Zhang, P. Cheng, B. Feng, W. Li, S. Sheng, H. Li, S. Meng, L. Chen, K. Wu, Metastable phases of 2D boron sheets on Ag(111), *Journal of Physics: Condensed Matter* 29 (9) (2017) 095002. doi:10.1088/1361-648X/aa5165.
- [18] Z. Zhang, E. S. Penev, B. I. Yakobson, Two-dimensional materials: Polyphony in b flat, *Nature Chemistry* 8 (2016) 525. doi:10.1038/nchem.2521.
- [19] P. Giannozzi, S. Baroni, N. Bonini, M. Calandra, R. Car, C. Cavazzoni, D. Ceresoli, G. L. Chiarotti, M. Cococcioni, I. Dabo, A. Dal Corso, S. de Gironcoli, S. Fabris, G. Fratesi, R. Gebauer, U. Gerstmann, C. Gougoussis, A. Kokalj, M. Lazzeri, L. Martin-Samos, N. Marzari, F. Mauri, R. Mazzarello, S. Paolini, A. Pasquarello, L. Paulatto, C. Sbraccia, S. Scandolo, G. Sclauzero, A. P. Seitsonen, A. Smogunov, P. Umari, R. M. Wentzcovitch, QUANTUM ESPRESSO: a modular and open-source software project for quantum simulations of materials, *Journal of Physics: Condensed Matter* 21 (2009) 395502. doi:10.1088/0953-8984/21/39/395502.
- [20] K. Momma, F. Izumi, VESTA3 for three-dimensional visualization of crystal, volumetric and morphology data, *Journal of Applied Crystallography* 44 (2011) 1272. doi:10.1107/S0021889811038970.
- [21] H. T. Stokes, D. M. Hatch, FINDSYM: program for identifying the space-group symmetry of a crystal, *Journal of Applied Crystallography* 38 (2005) 237. doi:10.1107/S0021889804031528.
- [22] C. Özdoğan, S. Mukhopadhyay, W. Hayami, Z. B. Güvenç, R. Pandey, I. Boustani, The unusually stable B₁₀₀ fullerene, structural transitions in boron nanostructures, and a comparative study of α - and γ -boron and sheets, *The Journal of Physical Chemistry C* 114 (10) (2010) 4362–4375. doi:10.1021/jp911641u.
- [23] M. Amsler, S. Botti, M. A. L. Marques, S. Goedecker, Conducting boron sheets formed by the reconstruction of the α -boron (111) surface, *Physical Review Letters* 111 (2013) 136101. doi:10.1103/PhysRevLett.111.136101.
- [24] H. Liu, J. Gao, J. Zhao, From boron cluster to two-dimensional boron sheet on cu(111) surface: Growth mechanism and hole formation 3 (2013) 3238, article. doi:10.1038/srep03238.
- [25] Y. Liu, E. S. Penev, B. I. Yakobson, Probing the synthesis of two-dimensional boron by first-principles computations, *Angewandte Chemie International Edition* 125 (11) (2013) 3238–3241. doi:10.1002/ange.201207972.
- [26] Z. Zhang, Y. Yang, G. Gao, B. I. Yakobson, Two-dimensional boron monolayers mediated by metal substrates, *Angewandte Chemie International Edition* 54 (44) (2015) 13022–13026. doi:10.1002/anie.201505425.
- [27] M. Topsakal, S. Ciraci, Static charging of graphene and graphite slabs, *Applied Physics Letters* 98 (13) (2011) 131908. doi:10.1063/1.3573806.
- [28] N. Y. Dzade, K. O. Obodo, S. K. Adjokatsé, A. C. Ashu, E. Amankwah, C. D. Atiso, A. A. Bello, E. Igumbor, S. B. Nzabarinda, J. T. Obodo, A. O. Ogbuu, O. E. Femi, J. O. Udeigwe, U. V. Waghmare, Silicene and transition metal based materials: prediction of a two-dimensional piezomagnet, *Journal of Physics: Condensed Matter* 22 (2010) 375502. doi:10.1088/0953-8984/22/37/375502.